PHYSICAL REVIEW C **87**, 051305(R) (2013)

Proton pair correlations and the neutrinoless double-β decay of ^{76}Ge

A. Roberts,[1,*] A. M. Howard,[1] J. J. Kolata,[1] A. N. Villano,[2] F. D. Becchetti,[3] P. A. DeYoung,[4] M. Febbraro,[3] S. J. Freeman,[5] B. P. Kay,[6,†] S. A. McAllister,[5] A. J. Mitchell,[5,‡] J. P. Schiffer,[7] J. S. Thomas,[5] and R. O. Torres-Isea[3]

[1]*Department of Physics, University of Notre Dame, Notre Dame, Indiana 46556, USA*
[2]*Department of Physics, University of Minnesota, Minneapolis, Minnesota 55455, USA*
[3]*Department of Physics, University of Michigan, Ann Arbor, Michigan 48109, USA*
[4]*Department of Physics, Hope College, Holland, Michigan 49422, USA*
[5]*School of Physics and Astronomy, University of Manchester, Manchester, M13 9PL, United Kingdom*
[6]*Department of Physics, University of York, York, YO10 5DD, United Kingdom*
[7]*Physics Division, Argonne National Laboratory, Argonne, Illinois 60439, USA*

(Received 25 April 2013; published 28 May 2013)

Proton pair correlations relevant for the neutrinoless double-β decay of ^{76}Ge have been probed via the ^{74,76}Ge(^{3}He,n) reactions at 16 MeV. No evidence for pairing vibrations in either nucleus is observed at sensitivity limits of $\sim$6% and $\sim$19% of the ground-state strength in ^{76}Se and ^{78}Se, respectively. These results are relevant for the understanding of matrix elements for neutrinoless double-β decay. The lack of pairing vibrations is consistent with a simple BCS structure for the ground states of ^{76}Ge and ^{76}Se, assumed in quasiparticle random phase approximation (QRPA) models of the process.

DOI: 10.1103/PhysRevC.87.051305 PACS number(s): 23.40.−s, 25.40.Hs, 27.50.+e

A concerted international effort is underway to experimentally measure neutrinoless double-β decay ($0\nu2\beta$) [1,2]. If observed, the Majorana nature of the neutrino would be confirmed, establishing it to be its own antiparticle. Moreover, a measurement of the decay rate would provide a means of accessing the effective neutrino mass but only if the nuclear matrix element for the transition is known. There is no other related process that contains this matrix element in the way that charge-exchange reactions, for instance, are related to the matrix elements for simple β decay. As such a direct experimental measurement of this quantity is not possible.

Calculation of the matrix element is also difficult. The short-ranged interactions involved in $0\nu2\beta$ result in large momentum transfer, permitting virtual intermediate states up to 100 MeV excitation to participate in the decay. The vast model space which results inhibits shell-model-based calculations. To handle this complexity the quasiparticle random phase approximation (QRPA) is frequently introduced [3]. While capable of accommodating the required model space, the QRPA relies upon a number of simplifying assumptions. Among these is that the initial and final states of the decaying system are well described as BCS condensates, requiring that all valence nucleons contribute coherently to the ground state.

The presence of "pairing vibrations" [4] indicates a breaking of this assumption. These form where gaps in the single-particle levels exist with energies greater than that associated with the pairing interaction. Nucleons in levels above the gap do not contribute to the ground-state condensate and instead form separate, pair-correlated excited states. The transfer cross section for $S = 0$ pairs of identical nucleons into these correlated states is greatly enhanced over noncorrelated states and provides a clear experimental signature of pairing vibrations. It is important to note that the proton-pairing structure need not reflect the neutron-pairing structure. This is well illustrated by pair-transfer studies on the $0\nu2\beta$ candidate ^{130}Te. No evidence is found from (p,t) reactions for pair vibrations in neutron-pair removal [5], but the proton-pair adding (^{3}He,n) measurements populated excited 0^+ states carrying $\sim$40% of the ground-state strength [6].

The $0\nu2\beta$-decay candidate ^{76}Ge has attracted considerable interest. Searches for $0\nu2\beta$ decay in ^{76}Ge have already begun [7], and it will also form the core of the upcoming MAJORANA and GERDA projects [8,9]. In recent years precision measurements of valence occupancies in the ^{76}Ge and ^{76}Se ground states have been reported [10,11], helping to constrain matrix element calculations. The neutron-pairing structure has also been tested [12], with no evidence for pair vibrations found. However, no such data currently exist for proton pairing. In this work we report on measurements relative to this $0\nu2\beta$ candidate using the (^{3}He,n) reaction as a probe.

Isotopically enriched targets of ^{74,76}Ge were bombarded with a 16 MeV ^{3}He beam provided by the Notre Dame tandem accelerator. To permit time-of-flight (TOF) measurements the beam was bunched with a width of $\sim$1 ns at the target position. Three of every four bunches were swept away to provide a time period of 406 ns which prevented the wraparound of low-energy neutrons over the long flight path used.

The areal density of the two targets was measured via Rutherford backscattering (RBS)[1] following the experiment.

*Present address: Los Alamos National Laboratory, PO Box 1663, MS H846, Los Alamos, New Mexico 87545.
†Present address: Physics Division, Argonne National Laboratory, Argonne, Illinois 60439, USA.
‡Present address: Department of Physics and Applied Physics, University of Massachusetts Lowell, Lowell, Massachusetts 01854, USA.

[1]The RBS measurements were done at Hope College in the Hope Ion Beam Analysis Lab. Email deyoung@hope.edu or peaslee@hope.edu for information about the facility.

Values of 1008 and 770 μg/cm^2 were obtained for ^{74}Ge and ^{76}Ge, respectively. Both targets were mounted onto 1 mg/cm^2 Au backing foils for support. During target irradiation the backing foils were orientated downstream to minimize the ^{3}He energy spread within the Ge layers. The isotopic purity of the target material was 99% for ^{74}Ge and 93% for ^{76}Ge.

The targets were mounted in a cylindrical, stainless-steel scattering chamber of radius 10 cm and wall thickness 0.2 cm. The total beam current delivered was measured by a Faraday cup situated behind the target. Both ^{74}Ge and ^{76}Ge targets were irradiated with an average beam current of 14 pnA for integrated exposure times of 2.81×10^5 s and 2.04×10^5 s, respectively. A Si surface-barrier detector, mounted at 45° relative to the beam axis, was used to monitor the target composition through elastically scattered ^{3}He ions. The detector resolution was sufficient to separate scattering from Ge and Au. The ratio of scattered ^{3}He to integrated beam current was found to be constant for each target throughout the experiment, indicating negligible change in the target properties.

The quality of the beam bunching at the target location was monitored by a BaF_2 detector positioned outside of the scattering chamber. The time interval between prompt γ-ray flashes, induced by beam interactions with the target, and the buncher timing signal was measured using a time-to-analog converter. The peak width in the resulting time spectrum provided a continuous measurement of the bunch width at the target position. To minimize neutron broadening of the spectrum the BaF_2 detector was mounted at a backward angle of ∼110° and shielded with 5 cm of paraffin.

The TOF of the outgoing fast neutrons was measured over a 14.6 m path length using the neutron wall at Notre Dame. The wall comprises 16 vertically mounted plastic-scintillator bars with dimensions 1.5 m × 0.15 m × 0.05 m. Each bar is instrumented with a fast rise-time photomultiplier tube (PMT) at either end, enabling an average time signal to be constructed and thereby eliminating uncertainty in the TOF due to the interaction location along the bar. Each PMT signal is amplified and fanned out into two channels. One channel is passed through a fast constant-fraction discriminator (CFD), and the resulting logic pulse compared to the buncher timing signal in a time-to-digital converter (TDC). The remaining channel is integrated using a charge-to-digital (QDC) converter to provide a measure of the energy deposition within the bar. A complete description of the neutron wall is given in Ref. [13].

The scintillator bars were arranged to span an angular range between 6° and 22° relative to the beam axis. Although the $\ell = 0$ cross section is peaked at 0°, angles below ∼6° were experimentally inaccessible due to the location of a concrete support pillar along the 0° axis. Furthermore, distorted-wave Born approximation (DWBA) calculations indicate that at ∼20° the $\ell = 0$ cross section will reach a minimum while the $\ell = 2$ cross section will be maximal. The distinctive $\ell = 0$ distribution across the angles covered permitted any 0^+ strength to be unambiguously identified.

The target-to-detector distance used is the largest permitted by the room geometry, corresponding to the best recoil-excitation resolution attainable. A byproduct of the large flight path is a reduction in the solid angle subtended by each element of the neutron wall and consequently an increased background rate relative to signal. The statistical fluctuation of this background is the limiting factor with respect to measuring weakly populated states, hence steps to minimize it are necessary. The primary background sources are γ-ray emissions from concrete in the room and high-energy muons produced by cosmic-ray interactions in the upper atmosphere. The photon background is reduced via cuts on the minimum energy deposition in each scintillator bar. By placing a cut at 7.2 MeV electron equivalent energy (MeVee), well above the thorium γ-ray edge, the photon background is largely eliminated, at the cost of a ∼50% reduction in efficiency for neutrons in the 20–26 MeV range. To reduce the muon background a veto shield has been designed and integrated into the wall. The shield consists of 1 cm thick scintillating paddles which provide 90% geometric coverage. When operated in anticoincidence mode the veto shield was found to reduce the remaining background by a factor of ten, consistent with a ∼100% intrinsic efficiency for muon detection, with negligible degradation of the neutron signal. The remaining background is composed predominantly of those muons whose trajectories bypass the veto shield. A full description of the muon shield can be found in Ref. [14].

Relative TOF spectra for each scintillator bar are produced by taking an average of the top- and bottom-TDC signals. An absolute timing calibration is determined using a high-precision, variable-frequency pulse generator. The precise flight path between the center of each element and the target was determined by a laser range finder to a precision of <0.1%. A time-zero calibration is thereafter provided by the arrival of the prompt γ-ray peak in each detector.

Forward-angle TOF spectra are shown in Fig. 1 for the population of states in ^{76}Se and ^{78}Se. The timing width of the ground-state peaks is 1.2 ns, which corresponds to an excitation-energy resolution of ∼300 keV. An asymmetric broadening of the peak base is observed, however, as a consequence of the non-Gaussian time structure of the bunched beam. The limiting factors on the time resolution are the width of the beam bunches impinging on the target (1 ns), ^{3}He energy loss within the target (0.3 ns), the transit time of neutrons through the scintillator bars (0.4 ns), and the timing response of the PMTs coupled to the fast CFDs (<1 ns). The carbon and oxygen contaminant peaks occur at excitation energies greater than 10 MeV in Se for both targets studied and therefore have negligible impact on the analysis.

Both spectra are characterized by a strongly populated ground state in close proximity to a broad continuum of unresolved states. Similar features have also been observed in (^{3}He,n) studies of the Cr, Fe, Ni, and Zn nuclei [15] where it was noted that the energy separation of the continuum from the ground state decreased with increasing reaction Q value. This trend is found to extend to the ^{76,78}Se nuclei with the onset of both continua occurring at ∼1 MeV excitation. The inferior peak-to-background ratio observed in the ^{78}Se data is a consequence of the thinner ^{76}Ge target used in addition to lower transfer cross sections owing to a less favorable reaction Q value. The consequence of this is a less stringent limit on excited 0^+ strength, as will be discussed below.

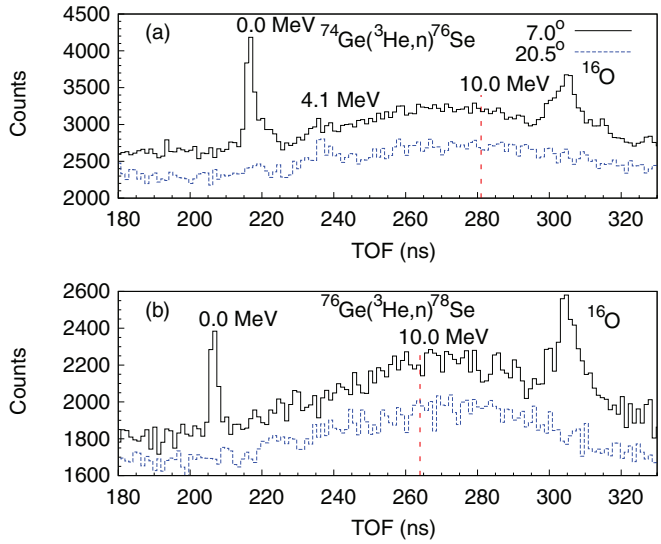

FIG. 1. (Color online) Neutron time-of-flight spectra for (a) ^{74}Ge(^{3}He,n)^{76}Se and (b) ^{76}Ge(^{3}He,n)^{78}Se. Summed spectra from the three most-forward and -backward scintillator bars are shown, each covering a total angular range of ∼2° centered around the angle indicated. The back-angle spectra are uniformly reduced by 500 and 300 counts in (a) and (b), respectively, for ease of display. The arrival of neutrons from contaminant groups occurs above 10 MeV excitation in both cases.

Low-lying 2^+ states are known in both ^{76,78}Se at ∼600 keV excitation. Neither of these states are resolved, however, due to the far greater yield, and broadened base, of the ground-state transition. Yields are therefore extracted for the unresolved $0^+_{\text{g.s.}} + 2^+$ doublet. The time-independent background upon which the peak sits is well constrained by the region of the TOF spectra between the arrival of the γ flash and the ground-state neutrons. The total number of counts is then the integrated yield of the peak, less the background contribution, with an overall uncertainty dominated by the statistical fluctuation of the background.

Translating the extracted yield into a cross section requires the neutron detection efficiency to be known. Efficiencies for the scintillator bars have been calculated up to energies of 28 MeV using a Monte Carlo approach described in Ref. [16]. These calculations require the PMT threshold and resolution as input and have been verified against known cross sections in the $d(d, n)$ reaction for energies up to 12 MeV and against 28 MeV neutrons from the ^{26}Mg(^{3}He,n) reaction [14]. In both cases the efficiency calculated was in agreement with that measured to within 10% percent.

Cross sections for the $0^+_{\text{g.s.}} + 2^+$ doublet are given as a function of angle in Table I. A systematic uncertainty in the cross section of ∼10% is estimated, dominated by the uncertainty in detection efficiency (<10%) and target thickness (<2%). At more backward angles groups of four scintillator bars are summed to improve the peak statistics. The same data are presented as angular distributions in Fig. 2, together with DWBA predictions for a $\ell = 0 + 2$ doublet. DWBA calculations were performed using the finite-range code FRESCO [17] assuming the nonlocal transfer of a bound diproton and use a postform with no remnant. The ^{3}He optical potential of Ref. [18] was used, and for the outgoing neutron the potential of Ref. [19] was adopted. The diproton wave function was assumed to have a single node in ^{3}He and four nodes when bound in Se. Both the optical and bound-state potentials are summarized in Table II.

TABLE I. Measured cross sections for population of the $0^+_{\text{g.s.}} + 2^+$ doublet in ^{76,78}Se. The uncertainties given are statistical only. An additional systematic uncertainty of ∼10% is estimated.

c.m. angle (deg)	^{76}Se (mb/sr)	^{78}Se (mb/sr)
6.2	259 ± 13	187 ± 23
7.0	242 ± 13	175 ± 22
7.8	239 ± 15	146 ± 25
8.6	185 ± 16	126 ± 26
10.8	139 ± 14	76 ± 24
11.5	127 ± 13	113 ± 22
12.2	112 ± 15	123 ± 25
12.9	72 ± 11	43 ± 19
16.4	39 ± 14	55 ± 12
21.0	32 ± 13	18 ± 11

Only a single excited state is clearly resolved in either nucleus, occurring at an excitation of 4.1(1) MeV in ^{76}Se. With reference to Fig. 1, the peak is observed to persist, and indeed strengthen, toward more backward angles indicating dominant $\ell \geqslant 1$ character. The observation of additional states is clearly limited, however, by statistical fluctuations within the background. An assessment of the sensitivity to excited states has been performed by considering the yield required for a peak to have a significance of at least 2σ above the background. The background level was determined by stepping a 7 ns integration window, within which 95% of the ground-state yield can be encompassed, across the TOF spectra formed from the three forward-most scintillator bars.

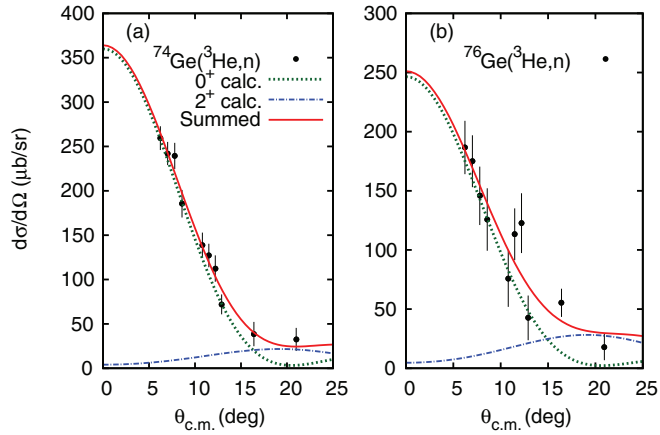

FIG. 2. (Color online) Comparison of measured ground-state and first-excited-state doublet cross section with DWBA calculations for a 0^+ plus 2^+ transition for reactions on (a) ^{74}Ge and (b) ^{76}Ge. Details of the DWBA calculations are in the text. Note that the two most-backward points are the summation of four evenly spaced scintillator bars, centered on the given angle.

TABLE II. Optical and bound-state potentials used in the DWBA analysis. See the text for details of the calculations. Both optical potentials vary slowly with N, Z, and E; the values given here are typical. Potentials are in MeV and radii in fm.† Adjusted on a state-by-state basis to reproduce the experimentally measured binding energy.

Particle	V	r	a	V_{SO}	r_{SO}	a_{SO}	W	r_W	a_W	W_D	r_{WD}	a_{WD}	W_{SO}	r_{WSO}	a_{WSO}	r_c
^{3}He	157.1	1.20	0.72	2.50	1.20	0.72	43.4	1.40	0.88							1.30
n	45.27	1.21	0.54	5.57	1.03	0.59	1.18	1.21	0.54	6.76	1.34	0.53	−0.07	1.03	0.59	
^{3}He bound state	†	1.175	0.65													
Se bound state	†	1.30	0.65													1.30

A quantitative comparison of the 0^+ sensitivity at different excitations requires that the neutron detection efficiency and Q-value dependence of the 0^+ cross section be factored out. The detection efficiency is well known as a function of energy, as discussed earlier, and changes only slowly over the range of neutron energies of interest in this work. The Q-value dependence of the cross section was assessed via DWBA calculations using the same methodology as described previously. As the reaction Q value is decreased, the matching for $\ell = 0$ transfer improves, increasing the calculated cross sections and hence improving the sensitivity limit as a function of excitation energy.

Calculated sensitivity limits, expressed as a percentage of the ground-state strength, are shown in Fig. 3 as a function of excitation energy. The ground-state cross section is adjusted from those in Table I to account for the small contribution of 2^+ strength. At the forward angles of interest this contribution is small and the uncertainty introduced by the correction is less than that of the statistical fluctuations in the yield. Limits on the sensitivity are cut off below 1 MeV excitation energy owing to the persistence of the ground-state peak. However, there is no evidence in the literature for 0^+ excitations below this energy [20]. The comparatively worse sensitivity for states in ^{78}Se is a consequence of the thinner ^{76}Ge target used together with lower transfer cross sections.

Data exist for proton-pair transfer on several other nuclei within the fpg shell. An additional consistency check of the results obtained in this work may be made through comparison of the measured ground-state cross sections with these other

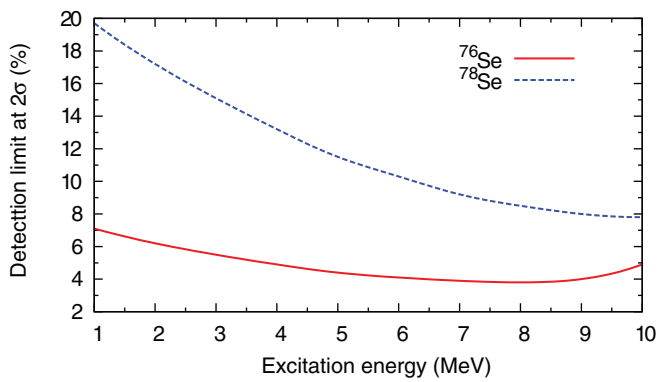

FIG. 3. (Color online) Detection limit for 0^+ strength relative to ground state for ^{74}Ge(^{3}He,n)^{76}Se and ^{76}Ge(^{3}He,n)^{78}Se. The curves have been corrected for the scintillator efficiency and Q-value dependence of the reaction (see text for details).

systems. Measured 0° cross sections for populating the ground states in ^{60,62,64,66}Zn [15] and ^{90}Zr [21] are shown in Fig. 4, together with data points for ^{76,78}Se from the present work. Since 0° measurements were not made in the present work, the cross sections given are those expected from the fits in Fig. 2. Also shown are corresponding DWBA calculations for each of the systems, again using the same methodology described earlier which serves to factor out the differences in bombarding energy and Q value. The isospin coupling, most significant for the Ni isotopes, is included for the DWBA values in Fig. 4. However, we note that the same spectroscopic factor is used in these calculations, while simple pairing theory would predict a factor of ∼2 increase in Ge relative to Ni. The microscopic contributions from $1p$ relative to $0f_{5/2}$ pairs would also cause changes at the factor-of-two level and may be in the opposite direction [22].

The calculations have been repeated for several potentials to assess the impact of optical-model choice on the analysis. With reference to Fig. 4, the choice of ^{3}He potential is found to have relatively little impact on the overall trend across the fpg isotopes plotted, although the GDP08 potential [23] is found to significantly over predict the ^{90}Zr cross section. The under prediction of the ^{60}Zn cross section may be a consequence of the increased contribution of the $1p$ orbital, as discussed above.

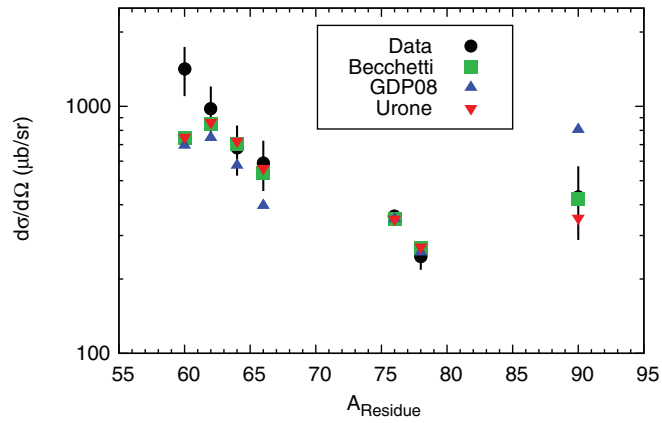

FIG. 4. (Color online) Ground-state cross sections for (^{3}He,n) reactions on fpg-shell nuclei. The results of DWBA calculations, normalized to the ^{76}Se measurement from this work and including the isospin coupling of $C^2 = (2T + 1)/(2T - 1)$, are shown for comparison. Results obtained with the GDP08 [23] and Urone *et al.* [25] ^{3}He potentials are also plotted. The error shown for ^{76}Se is statistical only and for ^{78}Se has the relative systematic error included (∼4%). All other points have their quoted systematic errors included.

A similar level of consistency was found when repeating the analysis using the neutron potential of Becchetti and Greenlees [24]. While changing the parametrization of the bound-state radii is found to have a strong effect on the magnitude of the calculated distributions, relative cross sections are found to be consistent to within a few percent at angles less than 20°.

Proton-pair creation onto ^{76}Ge has been explored using the (^{3}He,n) reaction on ^{74}Ge as well as ^{76}Ge. The change in ground-state cross section from ^{74}Ge to ^{76}Ge targets is basically a Q-value dependence that is well described by the DWBA. Therefore, the ground-state pairing in these two isotopes appears to be quite similar. No evidence for the breaking of the BCS approximation for paired protons in the Ge-Se region is seen, with a limit as low as 5%–7% below 4 MeV excitation energy.

We wish to thank John Greene of Argonne National Laboratory for his careful preparation of the Ge targets used in these measurements and the operating staff of the Nuclear Science Laboratory at Notre Dame. We also wish to thank Dr. Graham Peaslee of Hope College for his kind assistance with the RBS measurements. This work was supported in part by the National Science Foundation under Grant No. PHY09-69456, the US Department of Energy, Office of Nuclear Physics, under Contract No. DE-AC02-06CH11357, and the UK Science and Technology Facilities Council.

[1] B. Schwingenheuer, J. Phys.: Conf. Ser. **375**, 042007 (2012).
[2] V. M. Hannen, J. Phys.: Conf. Ser. **375**, 042004 (2012).
[3] S. R. Elliott and P. Vogel, Annu. Rev. Nucl. Sci. **52**, 115 (2002).
[4] R. Broglia, O. Hansen, and C. Riedel, in *Advances in Nuclear Physics*, edited by M. Baranger and E. Vogt (Springer, US, 1973), Vol. 6, pp. 287–457.
[5] T. Bloxham *et al.*, Phys. Rev. C **82**, 027308 (2010).
[6] W. P. Alford *et al.*, Nucl. Phys. A **323**, 339 (1979).
[7] M. Günther *et al.*, Phys. Rev. D **55**, 54 (1997).
[8] C. A. Ur, Nucl. Phys. B, Proc. Suppl. **217**, 38 (2011).
[9] C. E. Aalseth *et al.*, Nucl. Phys. B, Proc. Suppl. **217**, 44 (2011).
[10] J. P. Schiffer *et al.*, Phys. Rev. Lett. **100**, 11250 (2008).
[11] B. P. Kay *et al.*, Phys. Rev. C **79**, 021301 (2009).
[12] S. J. Freeman *et al.*, Phys. Rev. C **75**, 051301 (2007).
[13] J. J. Kolata *et al.*, Nucl. Instrum. Methods Phys. Res., Sect. A **557**, 594 (2006).
[14] A. Roberts, Ph.D. thesis, University of Notre Dame, 2013; A. Roberts *et al.*, (unpublished).
[15] W. P. Alford *et al.*, Nucl. Phys. A **243**, 269 (1975).
[16] R. A. Cecil, B. D. Anderson, and R. Madey, Nucl. Instrum. Methods **161**, 439 (1979).
[17] I. J. Thompson, Comput. Phys. Rep. **7**, 167 (1988).
[18] F. D. Becchetti, W. Makofske, and G. W. Greenlees, Nucl. Phys. A **190**, 437 (1972).
[19] A. J. Koning and J. P. Delaroche, Nucl. Phys. A **713**, 231 (2003).
[20] A. R. Farhan, Nucl. Data Sheets **74**, 529 (1995); B. Singh and D. A. Viggars, *ibid.* **42**, 233 (1984).
[21] H. W. Fielding *et al.*, Nucl. Phys. A **269**, 125 (1976).
[22] B. F. Bayman, Phys. Rev. Lett. **25**, 1768 (1970).
[23] D. Y. Pang, P. Roussel-Chomaz, H. Savajols, R. L. Varner, and R. Wolski, Phys. Rev. C **79**, 024615 (2009).
[24] F. D. Becchetti and G. W. Greenlees, Phys. Rev. **182**, 1190 (1969).
[25] P. P. Urone *et al.*, Nucl. Phys. A **163**, 225 (1971).